THE EUROPEAN
PHYSICAL JOURNAL C

# When energy goes missing: new physics in $b \to s\nu\nu$ with sterile neutrinos

**Tobias Felkl**[1] [iD], **Anjan Giri**[2] [iD], **Rukmani Mohanta**[3] [iD], **Michael A. Schmidt**[1,a] [iD]

[1] Sydney Consortium for Particle Physics and Cosmology, School of Physics, The University of New South Wales, Sydney, NSW 2052, Australia
[2] Department of Physics, IIT Hyderabad, Kandi 502285, India
[3] School of Physics, University of Hyderabad, Hyderabad 500046, India

**Abstract** Belle II recently reported the first measurement of $B^+ \to K^+ + \text{inv}$, which is $2.8\sigma$ above the Standard Model prediction. We explore the available parameter space of new physics within Standard Model effective field theory extended by sterile neutrinos ($\nu$SMEFT) and provide predictions for the other $B \to K^{(\star)} + \text{inv}$ decay modes and invisible $B_s$ decays. We also briefly comment on charged current decays $B \to D^{(\star)}\ell\bar{\nu}$ and possible ultraviolet completions of the relevant $\nu$SMEFT operators.

## 1 Introduction

The Belle II experiment recently announced the first measurement of $B^+ \to K^+ + \text{inv}$ with a branching ratio of $\text{BR}(B^+ \to K^+ + \text{inv}) = (2.4 \pm 0.7) \times 10^{-5}$ [1], which is $2.8\sigma$ above the Standard Model (SM) prediction $\text{BR}(B^+ \to K^+\nu\bar{\nu})_{\text{SM}} = (5.06 \pm 0.14 \pm 0.28) \times 10^{-6}$ [2]. The result assumes 3-body decay kinematics as predicted by the SM and is based on two independent analyses, one inclusive analysis and one with a hadronic tag. While the hadronic tag analysis is consistent with the SM prediction within $1\sigma$, the more sensitive inclusive tag analysis shows a $3\sigma$ deviation from the SM prediction. Together with the previous searches by Belle [3,4], BaBar [5] and Belle II [6], a simple weighted average results in $\text{BR}(B^+ \to K^+ + \text{inv}) = (1.4 \pm 0.4) \times 10^{-5}$ [1]. Motivated by the result, Refs. [7,8] studied the implication within Standard Model effective field theory (SMEFT) and Ref. [9] demonstrated that non-universal lepton-flavour-conserving $Z'$ models are not able to accommodate the excess and thus proposed the introduction of lepton-flavour-violating couplings. Several earlier works [10–15] also proposed explanations for an excess in

$B^+ \to K^+ + \text{inv}$ motivated by the result of the 2021 Belle II analysis [6], which first used the inclusive tagging method.

One attractive explanation of the excess in $B^+ \to K^+ + \text{inv}$ is an additional decay channel with undetected final states, like sterile neutrinos [11,12], dark matter [13,16,17] or more generally long-lived particles [14,18–22]. Additional light sterile neutrinos are particularly well motivated, and occur in numerous minimal extensions of the SM, see e.g. [23–28]. Light sterile neutrinos have been proposed as an explanation of the deviation from lepton flavour universality in $R(D^{(\star)})$ [25,29–35] by introducing new decay channels, $B \to D^{(\star)}\tau N$, with sterile neutrinos $N$. Light GeV-scale sterile neutrinos may also explain neutrino masses via the seesaw mechanism [36] like in the $\nu$MSM [37]. The lifetime of sterile neutrinos is constrained from big bang nucleosynthesis (BBN) to be shorter than 0.02 s [38]. Together with searches for sterile neutrinos at beam dump experiments, this translates into a lower bound on their mass in the minimal seesaw model of $\mathcal{O}(350)$ MeV apart from a small mass window at 120–140 MeV [39]. Although the lower bound is well below the $B^+$ meson mass, the sterile neutrino mass will become important for a relevant part of the parameter space and thus should be included in the analysis.

$B$ meson decays are best described within low energy effective theory (LEFT). Most studies focus on vector operators [17,40–42], because they are predicted in the SM, but sterile neutrinos motivate to extend the analysis to scalar and tensor operators. The scenario of massless sterile neutrinos has been discussed in [7,10,43–45] and the general case with massive neutrinos has been considered by some of us in [12] in terms of helicity amplitudes [46]. There are also recent studies of $B \to K^{(\star)}\nu\bar{\nu}$ decays within SMEFT, which discuss the complementarity with other observables [7,45,47] including comments on scalar operators with (massless) right-handed neutrinos [7,45].

[a] e-mail: m.schmidt@unsw.edu.au (corresponding author)

Springer

In this work, we will build on a previous analysis within LEFT [12], but work within SM effective field theory extended by sterile neutrinos ($\nu$SMEFT). Within the framework of $\nu$SMEFT we consider additional decay channels to sterile neutrinos including the full sterile neutrino mass dependence and identify the viable regions of parameter space which explain the excess in $B^+ \to K^+ + \text{inv}$ and are consistent with the non-observation of the other three $B \to K^{(\star)} + \text{inv}$ decay modes, invisible $B_s$ decays and measurements of charged current $B \to D^{(\star)} \ell \bar{\nu}$ decays. We also point out ultraviolet (UV) completions for the viable $\nu$SMEFT operators.

The remainder of the paper is structured as follows. In Sect. 2 we introduce the effective field theory (EFT) framework, discuss both $\nu$SMEFT and LEFT and how they are connected via renormalisation group (RG) running. The relevant observables are introduced in Sect. 3 and the results discussed in Sect. 4. Finally, possible UV completions are presented in Sect. 5 before concluding in Sect. 6. A few technical details are relegated to the Appendix.

## 2 Effective field theory framework

Starting at dimension-6, there are operators in $\nu$SMEFT which contribute to $b \to s\nu\nu$ at tree level. We focus on the four semi-leptonic 4-fermion operators with sterile neutrinos [48]

$$
\begin{aligned}
\mathcal{L} &= C^{\mathrm{QN}}(\bar{Q}\gamma_\mu Q)(\bar{N}\gamma^\mu N) + C^{\mathrm{dN}}(\bar{d}\gamma_\mu d)(\bar{N}\gamma^\mu N) \\
&\quad + C^{\mathrm{LNQd}}(\bar{L}^\alpha N)\epsilon_{\alpha\beta}(\bar{Q}^\beta d) \\
&\quad + C^{\mathrm{LNQdT}}(\bar{L}^\alpha \sigma^{\mu\nu} N)\epsilon_{\alpha\beta}(\bar{Q}^\beta \sigma_{\mu\nu} d),
\end{aligned}
\tag{1}
$$

where $Q$, $L$ and $d$ are the SM left-handed quark doublet, left-handed lepton doublet and right-handed down-type quark singlet, respectively, and $N$ denotes right-handed neutrinos, i.e. right-handed SM singlet fermions. Flavour and colour indices are suppressed, $\sigma^{\mu\nu} = \frac{i}{2}[\gamma^\mu, \gamma^\nu]$ and the Levi-Civita tensor is defined with $\epsilon_{12} = 1$. Assigning lepton number $+1$ to $N$, all four operators are lepton number conserving. In contrast to [48], we introduce a tensor operator. This operator basis is convenient as $\mathcal{O}^{\mathrm{LNQd}}$ and $\mathcal{O}^{\mathrm{LNQdT}}$ do not mix under 1-loop QCD renormalisation group (RG) running. The tensor operator $\mathcal{O}^{\mathrm{LNQdT}}$ is related to the scalar operators in [48] via a Fierz transformation

$$
\begin{aligned}
&(\bar{L}^\alpha \sigma^{\mu\nu} N)\epsilon_{\alpha\beta}(\bar{Q}^\beta \sigma_{\mu\nu} d) \\
&= -8(\bar{L}^\alpha d)\epsilon_{\alpha\beta}(\bar{Q}^\beta N) - 4(\bar{L}^\alpha N)\epsilon_{\alpha\beta}(\bar{Q}^\beta d).
\end{aligned}
\tag{2}
$$

For this analysis we define all $\nu$SMEFT operators at the scale $\mu = 1$ TeV. At the electroweak scale $\Lambda_{\mathrm{EW}} = m_Z$, the $\nu$SMEFT operators are matched onto LEFT.

Only a few operators in LEFT are generated at tree level from the set of $\nu$SMEFT operators introduced above. The relevant interactions for $b \to s\nu\nu$ and $b \to c\ell\nu$ processes are described by the Lagrangian [49,50]

$$
\begin{aligned}
\mathcal{L} &= \sum_{X=L,R} C^{\mathrm{VLX}}_{\nu d} \mathcal{O}^{\mathrm{VLX}}_{\nu d} + \Big( C^{\mathrm{SLL}}_{\nu d} \mathcal{O}^{\mathrm{SLL}}_{\nu d} + C^{\mathrm{TLL}}_{\nu d} \mathcal{O}^{\mathrm{TLL}}_{\nu d} \\
&\quad + C^{\mathrm{VLL}}_{\nu e d u} \mathcal{O}^{\mathrm{VLL}}_{\nu e d u} + C^{\mathrm{SLL}}_{\nu e d u} \mathcal{O}^{\mathrm{SLL}}_{\nu e d u} + C^{\mathrm{TLL}}_{\nu e d u} \mathcal{O}^{\mathrm{TLL}}_{\nu e d u} + \mathrm{h.c.} \Big)
\end{aligned}
\tag{3}
$$

with the effective operators

$$
\begin{aligned}
\mathcal{O}^{\mathrm{VLX}}_{\nu d} &= (\overline{\nu_L}\gamma_\mu \nu_L)(\overline{d_X}\gamma^\mu d_X), \\
\mathcal{O}^{\mathrm{SLL}}_{\nu d} &= (\overline{\nu_L^c}\nu_L)(\overline{d_R}d_L), \\
\mathcal{O}^{\mathrm{TLL}}_{\nu d} &= (\overline{\nu_L^c}\sigma_{\mu\nu}\nu_L)(\overline{d_R}\sigma^{\mu\nu}d_L), \\
\mathcal{O}^{\mathrm{VLL}}_{\nu e d u} &= (\overline{\nu_L}\gamma_\mu e_L)(\overline{d_L}\gamma^\mu u_L), \\
\mathcal{O}^{\mathrm{SLL}}_{\nu e d u} &= (\overline{\nu_L^c}e_L)(\overline{d_R}u_L), \\
\mathcal{O}^{\mathrm{TLL}}_{\nu e d u} &= (\overline{\nu_L^c}\sigma_{\mu\nu}e_L)(\overline{d_R}\sigma^{\mu\nu}u_L).
\end{aligned}
\tag{4}
$$

Right-handed neutrinos $N$ are expressed in terms of left-handed Weyl spinors $\nu_L = N^c \equiv C\overline{N}^T$ with the charge conjugation matrix $C = i\gamma^2\gamma^0$. SM neutrinos carry the generation index $\alpha = 1, 2, 3$ and sterile neutrinos are labelled with $\alpha \geq 4$.

Note that the scalar operator $\mathcal{O}^{\mathrm{SLL}}_{\nu d}$ is symmetric in the neutrino flavours and the tensor operator $\mathcal{O}^{\mathrm{TLL}}_{\nu d}$ is antisymmetric in the neutrino flavours, which can be straightforwardly derived from

$$
\begin{aligned}
\overline{\psi_i^c}\Gamma\psi^{cj} &= \eta_\Gamma \overline{\psi^j}\Gamma\psi_i, \quad C^{-1}\Gamma C = \eta_\Gamma \Gamma^T, \\
\eta_\Gamma &= \begin{cases} +1 & \text{for } \Gamma = 1, \gamma_5, \gamma^\mu\gamma_5 \\ -1 & \text{for } \Gamma = \gamma^\mu, \sigma^{\mu\nu}, \sigma^{\mu\nu}\gamma_5 \end{cases}.
\end{aligned}
\tag{5}
$$

The other operators do not exhibit any manifest symmetry properties.[1]

The matching conditions have been obtained by translating the existing matching results in the literature [50–52] to the operator basis we are using. All LEFT operators are given in the mass eigenstate basis, while the

---

[1] There are further LEFT operators

$$
\begin{array}{ll}
\mathcal{O}^{\mathrm{SLR}}_{\nu d} = (\overline{\nu_L^c}\nu_L)(\overline{d_L}d_R) & \mathcal{O}^{\mathrm{VLR}}_{\nu e d u} = (\overline{\nu_L}\gamma_\mu e_L)(\overline{d_R}\gamma^\mu u_R) \\
\mathcal{O}^{\mathrm{SRL}}_{\nu e d u} = (\overline{\nu_L}e_R)(\overline{d_R}u_L) & \mathcal{O}^{\mathrm{VRL}}_{\nu e d u} = (\overline{\nu_L^c}\gamma_\mu e_R)(\overline{d_L}\gamma^\mu u_L) \\
\mathcal{O}^{\mathrm{SLR}}_{\nu e d u} = (\overline{\nu_L^c}e_L)(\overline{d_L}u_R) & \mathcal{O}^{\mathrm{VRR}}_{\nu e d u} = (\overline{\nu_L^c}\gamma_\mu e_R)(\overline{d_R}\gamma^\mu u_R) \\
\mathcal{O}^{\mathrm{SRR}}_{\nu e d u} = (\overline{\nu_L}e_R)(\overline{d_L}u_R) & \mathcal{O}^{\mathrm{TRR}}_{\nu e d u} = (\overline{\nu_L}\sigma_{\mu\nu}e_R)(\overline{d_L}\sigma^{\mu\nu}u_R)
\end{array}
\tag{6}
$$

that also contribute to bespoke processes, but are not induced via tree-level matching to the considered dimension-6 $\nu$SMEFT operators. They are however referenced in Appendix A where the mapping onto the $S, P, V, A, \mathcal{T}$ basis is presented.

operators in $\nu$SMEFT are defined in the interaction basis, where the charged leptons and down-type quarks are mass eigenstates. Up-type quark mass eigenstates $\hat{u}_i$ and neutrino mass eigenstates $\hat{\nu}_i$ are related to the interaction basis by

$$u_\alpha = (V^\dagger)_{\alpha i} \hat{u}_i, \qquad \nu_\alpha = U_{\alpha i} \hat{\nu}_i, \qquad (7)$$

where $V$ denotes the Cabibbo–Kobayashi–Maskawa (CKM) matrix, and $U$ is the leptonic mixing matrix. The top-left $3 \times 3$ sub-block of the leptonic mixing matrix $U$ is approximately given by the Pontecorvo–Maki–Nakagawa–Sakata (PMNS) matrix. For a large part of the parameter space, (sterile) neutrino masses are negligible compared to the $B$ meson mass, $m_\alpha \ll m_B$, and thus (sterile) neutrinos can be treated as massless and the PMNS matrix is unphysical in this limiting case. Even for sterile neutrinos with GeV-scale masses, CHARM [53], NuTeV [54] and DELPHI [55] constrain the active-sterile mixing to be small, $|U|^2 \lesssim 10^{-5}$, for the relevant region in parameter space. Thus, in the following we neglect leptonic mixing and treat the sterile neutrinos as mass eigenstates, and so drop the hats from the mass eigenstates for simplicity.

At tree level, we find the following non-vanishing down-quark flavour-violating Wilson coefficients for $b \to s\nu\nu$ processes and vector operators with $\alpha, \beta \geq 4$

$$
\begin{aligned}
C^{\text{VLL}}_{vd,\alpha\beta sb} &= -C^{\text{QN}}_{sb(\beta-3)(\alpha-3)}, \\
C^{\text{VLR}}_{vd,\alpha\beta sb} &= -C^{\text{dN}}_{sb(\beta-3)(\alpha-3)},
\end{aligned}
\qquad (8)
$$

and for the scalar and tensor operators

$$
\begin{aligned}
C^{\text{SLL}}_{vd,\alpha\beta sb} &= \begin{cases} \frac{1}{2} C^{\text{LNQd}*}_{\beta(\alpha-3)bs} & \alpha \geq 4;\ 1 \leq \beta \leq 3 \\ \frac{1}{2} C^{\text{LNQd}*}_{\alpha(\beta-3)bs} & 1 \leq \alpha \leq 3;\ \beta \geq 4 \end{cases}, \\
C^{\text{SLL}}_{vd,\alpha\beta bs} &= \begin{cases} \frac{1}{2} C^{\text{LNQd}*}_{\beta(\alpha-3)sb} & \alpha \geq 4;\ 1 \leq \beta \leq 3 \\ \frac{1}{2} C^{\text{LNQd}*}_{\alpha(\beta-3)sb} & 1 \leq \alpha \leq 3;\ \beta \geq 4 \end{cases}, \\
C^{\text{TLL}}_{vd,\alpha\beta sb} &= \begin{cases} \frac{1}{2} C^{\text{LNQdT}*}_{\beta(\alpha-3)bs} & \alpha \geq 4;\ 1 \leq \beta \leq 3 \\ -\frac{1}{2} C^{\text{LNQdT}*}_{\alpha(\beta-3)bs} & 1 \leq \alpha \leq 3;\ \beta \geq 4 \end{cases}. \\
C^{\text{TLL}}_{vd,\alpha\beta bs} &= \begin{cases} \frac{1}{2} C^{\text{LNQdT}*}_{\beta(\alpha-3)sb} & \alpha \geq 4;\ 1 \leq \beta \leq 3 \\ -\frac{1}{2} C^{\text{LNQdT}*}_{\alpha(\beta-3)sb} & 1 \leq \alpha \leq 3;\ \beta \geq 4 \end{cases}.
\end{aligned}
\qquad (9)
$$

Note, we explicitly (anti-)symmetrised the scalar (tensor) Wilson coefficients. Furthermore, at tree level the non-vanishing LEFT operators for $b \to c\ell\nu$ processes are given by scalar and tensor operators which are matched to $\nu$SMEFT operators

$$
\begin{aligned}
C^{\text{SLL}}_{vedu,\alpha\beta bc} &= -V^*_{cm} C^{\text{LNQd}*}_{\beta(\alpha-3)mb}, \\
C^{\text{TLL}}_{vedu,\alpha\beta bc} &= -V^*_{cm} C^{\text{LNQdT}*}_{\beta(\alpha-3)mb} \quad \text{with } \alpha \geq 4.
\end{aligned}
\qquad (10)
$$

In addition to the contribution from $\nu$SMEFT dimension-6 operators, the SM contribution to the LEFT operators relevant for $b \to s, c$ processes can be summarised as

$$
\begin{aligned}
C^{\text{VLL,SM}}_{vd,\alpha\beta sb} &= -\frac{4G_F}{\sqrt{2}} \frac{\alpha}{2\pi} V^*_{ts} V_{tb} \frac{X}{\sin^2\theta_w} \delta_{\alpha\beta}, \\
C^{\text{VLL,SM}}_{vedu,\alpha\beta bc} &= -\frac{4G_F}{\sqrt{2}} V^*_{cb} \delta_{\alpha\beta}
\end{aligned}
\qquad (11)
$$

in terms of the function $X$ [56]. The Wilson coefficient for $b \to s\nu\bar{\nu}$ includes electroweak corrections induced by top quarks at 2-loop order, which are numerically given by $X = 6.3772 \sin^2\theta_w$ [57–59].

The dominant RG corrections originate from strong interactions. While the (axial-)vector current operators do not receive QCD corrections at 1-loop order, scalar and tensor operators receive RG corrections. The 1-loop RG equations for the scalar and tensor Wilson coefficients $C^S$ and $C^T$ are

$$
\frac{d\ln C^S}{d\ln\mu} = -3C_F \frac{\alpha_s}{2\pi}, \qquad \frac{d\ln C^T}{d\ln\mu} = C_F \frac{\alpha_s}{2\pi}, \qquad (12)
$$

with the second Casimir invariant $C_F = (N_c^2 - 1)/2N_c = 4/3$ for $N_c = 3$ and $\alpha_s = g_s^2/4\pi$. Taking into account 1-loop QCD running, we arrive at

$$
\begin{aligned}
C^S(\mu_1) &= \left( \frac{\alpha_s(\mu_2)}{\alpha_s(\mu_1)} \right)^{3C_F/b} C^S(\mu_2), \\
C^T(\mu_1) &= \left( \frac{\alpha_s(\mu_2)}{\alpha_s(\mu_1)} \right)^{-C_F/b} C^T(\mu_2),
\end{aligned}
\qquad (13)
$$

where $b = -11 + \frac{2}{3} n_f$ and $n_f$ is the number of active quark flavours. As there is no operator mixing for 1-loop QCD running in the chosen operator basis, there is a one-to-one correspondence between a given LEFT Wilson coefficient at the hadronic scale $\mu = 4.8$ GeV and the $\nu$SMEFT Wilson coefficient at $\mu = 1$ TeV: All scalar LEFT operators are rescaled with the factor 1.608 and tensor operators with 0.853 compared to the result from matching $\nu$SMEFT to LEFT.

## 3 Phenomenology

Belle II measured [1] the decay $B^+ \to K^+ + \text{inv}$ with a branching ratio of $\text{BR}(B^+ \to K^+ + \text{inv}) = (2.4 \pm 0.7) \times 10^{-5}$ assuming a 3-body decay with massless neutrinos, which is above the 90% CL exclusion limit of $\text{BR}(B^+ \to K^+ + \text{inv}) < 1.6 \times 10^{-5}$ [5]. Together with the previous searches for $B^+ \to K^+ + \text{inv}$ [4,5,60], the Belle II measurement results in a simple weighted average of $\text{BR}(B^+ \to K^+ + \text{inv}) = (1.4 \pm 0.4) \times 10^{-5}$ [1]. The other searches for $B \to K^{(\star)} + \text{inv}$ so far only resulted in
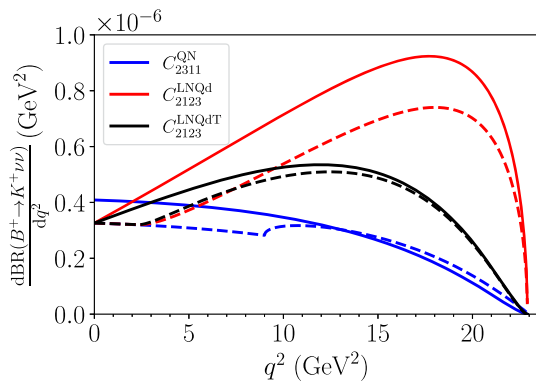
**Fig. 1** Differential branching ratio as a function of the missing invariant mass squared $q^2$ for vector (blue), scalar (red) and tensor (black) operators. All Wilson coefficients are fixed to $C = 0.01$ TeV$^{-2}$ at $\mu = 1$ TeV and the SM contribution is taken into account. The solid lines are for massless sterile neutrinos and the dashed line for a sterile neutrino of mass $m_1 = 1.5$ GeV

upper limits of BR($B^0 \rightarrow K^0 +$ inv) $< 2.6 \times 10^{-5}$ [4],[2] BR($B^0 \rightarrow K^{\star 0} +$ inv) $< 1.8 \times 10^{-5}$ [4], and BR($B^+ \rightarrow K^{\star +} +$ inv) $< 4.0 \times 10^{-5}$ [3].

The short-distance contributions to the differential decay rates of semi-leptonic $B$ meson decays are straightforwardly expressed in terms of helicity amplitudes

$$\frac{d\Gamma(\bar{B} \rightarrow \bar{K}\nu_\alpha\nu_\beta)}{dq^2} = \frac{1}{4(1+\delta_{\alpha\beta})}G^{(0)}(q^2),$$

$$\frac{d\Gamma(\bar{B} \rightarrow \bar{K}^\star(\rightarrow \bar{K}\pi)\nu_\alpha\nu_\beta)}{dq^2} = \frac{3}{4(1+\delta_{\alpha\beta})}G_0^{0,0}(q^2),$$

(14)

where the coefficients $G^{(0)}(q^2)$ and $G_0^{0,0}(q^2)$ of the Wigner-D functions are defined in [46] with the replacements for neutrinos as discussed in [12] and $q^2$ denotes the missing invariant mass squared carried away by the two neutrinos.[3] Kinematics constrains $q^2$ to lie in the range $(m_\alpha + m_\beta)^2 \leq q^2 \leq (m_{B^+} - m_{K^+})^2$. We use the recently published $B \rightarrow K^{(\star)}$ form factors from [61] with the parametrisation defined in [62]. Following [63], we increase the $B \rightarrow K^\star\nu\nu$ branching ratios by 20% to account for finite-width effects.

Note that massive sterile neutrinos and the Lorentz structure of the operators result in modifications to the $q^2$ distribution compared to the SM prediction, see e.g. [12], which is illustrated in Fig. 1 for $B^+ \rightarrow K^+\nu\nu$. The $q^2$ distributions of $B \rightarrow K^{(\star)}\nu\nu$ decays are also dependent on the sterile

neutrino mass and Lorentz structure of the operators. Heavy sterile neutrinos do not contribute below $q^2 < 4m_1^2$ for the vector operators $\mathcal{O}^{QN}$ and $\mathcal{O}^{dN}$ and $q^2 < m_1^2$ for scalar operators $\mathcal{O}^{LdQN}$ and tensor operators $\mathcal{O}^{LdQNT}$. Below the kinematic cutoff for sterile neutrinos, the dashed lines in Fig. 1 approach the SM prediction. In comparison to vector operators, scalar and tensor operators are enhanced for large $q^2$. The experimental efficiency however is largest for small $q^2$ and reduced for large $q^2$. As there is currently no publicly available $q^2$ distribution which could be used for recasting the Belle II result [1], we only consider branching ratios and do not take into account modifications to the $q^2$ distribution. Viable regions of parameter space which explain the branching ratio measured by Belle II can only be taken as indicative and we would like to stress the need for a more detailed discussion of sterile neutrino final states based on the full $q^2$ distribution.

In addition to the short-distance contribution, there is a long-distance tree-level contribution to $B^+ \rightarrow K^{(\star)+}\nu\bar{\nu}$ in the SM. [64] It is mediated by a $\tau$ lepton, $B^+ \rightarrow \tau^+(\rightarrow K^{(\star)+}\bar{\nu}_\tau)\nu_\tau$. The interference between the long-distance and short-distance contributions is negligible due to the narrow $\tau$ resonance [64] and thus the total branching ratio for $B^+ \rightarrow K^{(\star)+}\nu\bar{\nu}$ is approximately obtained by summing the short- and long-distance contributions. Although the long-distance contribution is subdominant, since it only amounts to about 10% of the short-distance contribution, we nevertheless include it in the numerical analysis.

Another relevant decay channel is the invisible decay of $B_s$ mesons. Reference [65] recently derived a first upper bound on the branching ratio of invisible $B_s$ decays using LEP data with BR($B_s \rightarrow$ inv) $< 5.9 \times 10^{-4}$. It may also be probed at the Belle II experiment: Using an integrated luminosity of 5 ab$^{-1}$ allows to probe BR($B_s \rightarrow$ inv) $> 1.1 \times 10^{-5}$ [66]. The branching ratio for identical final state neutrinos is given by

$$\text{BR}(B_s \rightarrow \nu_\alpha\nu_\alpha) = \frac{\tau_{B_s}m_{B_s}^3 f_{B_s}^2}{32\pi}$$

$$\times \left( \left| C_{vd,\alpha\alpha sb}^{\text{VLR}} - C_{vd,\alpha\alpha sb}^{\text{VLL}} \right|^2 x_\alpha^2\sqrt{1-4x_\alpha^2} \right.$$

$$+ \left| C_{vd,\alpha\alpha bs}^{\text{SLL}*} - C_{vd,\alpha\alpha sb}^{\text{SLL}} \right|^2 \frac{(1-4x_\alpha^2)^{3/2}}{4x_b^2}$$

$$+ \left| C_{vd,\alpha\alpha bs}^{\text{SLL}*} + C_{vd,\alpha\alpha sb}^{\text{SLL}} \right|^2 \frac{\sqrt{1-4x_\alpha^2}}{4x_b^2}$$

$$+ \text{Re}\left[ (C_{vd,\alpha\alpha sb}^{\text{VLR}} - C_{vd,\alpha\alpha sb}^{\text{VLL}})(C_{vd,\alpha\alpha bs}^{\text{SLL}} + C_{vd,\alpha\alpha sb}^{\text{SLL}*}) \right]$$

$$\left. \times \frac{x_\alpha\sqrt{1-4x_\alpha^2}}{x_b} \right),$$

(15)

---

[2] Reference [4] quotes the upper bound on the branching ratio for $B^0 \rightarrow K_S^0\nu\nu$ which we translated to $B^0 \rightarrow K^0\nu\nu$.

[3] Note, in contrast to [12], the symmetry factor $(1 + \delta_{\alpha\beta})$ for identical neutrinos has been explicitly included in the differential decay rate instead of the normalisation factor $N$.

with $x_\alpha = m_\alpha/m_{B_s}$ and $x_b = m_b/m_{B_s}$. The general expression for different neutrino final states is presented in App. B. Vector contributions are helicity suppressed and thus in the limit of vanishing sterile neutrino masses, there is only a contribution from scalar operators [7,45]

$$\mathrm{BR}(B_s \to \nu_\alpha \nu_\alpha) = \frac{\tau_{B_s} m_{B_s}^5 f_{B_s}^2}{64\pi m_b^2}$$
$$\times \left( \left| C_{vd,\alpha\alpha bs}^{\mathrm{SLL}} \right|^2 + \left| C_{vd,\alpha\alpha sb}^{\mathrm{SLL}} \right|^2 \right). \quad (16)$$

Directly related to the discussed processes are the rare decays $B_s \to \phi\nu\nu$ and $\Lambda_b \to \Lambda^{(\star)}\nu\nu$ which provide independent information. The differential branching ratio for $B_s \to \phi\nu\nu$ has the same form as the one for $B \to K^*\nu\nu$ with the form factors replaced by the $B_s \to \phi$ form factors presented in [61]. See [67] for a calculation in SMEFT. The differential branching ratio for $\Lambda_b \to \Lambda^{(\star)}\nu\bar{\nu}$ has been calculated in [68] within SMEFT. Within $\nu$SMEFT it may be obtained from the differential branching ratio for the rare $\Lambda_b$ decay with charged leptons, see [69], similar to the discussion of $B \to K^{(\star)}\nu\nu$ in [12]. These channels are inaccessible at the Belle II experiment running at the $\Upsilon(4S)$ resonance, but a Tera-Z experiment such as FCC-ee or CEPC may be able to measure these channels as pointed out in [70,71]. Given the uncertain experimental situation, we leave the discussion of these channels for future work. If the anomaly persists, it will be highly interesting to measure $B_s \to \phi\nu\nu$ and $\Lambda_b \to \Lambda^{(\star)}\nu\nu$ to pin down the Lorentz structure of the effective operators.

Additional constraints arise from light-lepton flavour universality ratios for charged current processes $b \to c\ell\bar{\nu}$. The differential branching ratios are obtained by exchanging $\nu_\alpha \to e_\alpha$ in Eq. (14) and dropping the factors $(1 + \delta_{\alpha\beta})$ for identical final state particles, see also [72]. The relevant form factors for $B \to D^{(\star)}$ are taken from [73]. Three different ratios have been measured: Belle measured $\frac{\mathrm{BR}(B \to D\mu\nu)}{\mathrm{BR}(B \to De\nu)} = 0.995 \pm 0.045$ [74] which is consistent with the SM prediction of 0.997. Similarly, the measurement of $\frac{\mathrm{BR}(B^0 \to D^{\star-}e^+\nu)}{\mathrm{BR}(B^0 \to D^{\star-}\mu^+\nu)} = 1.01 \pm 0.032$ by Belle [66] is consistent with the SM prediction of 1.005. Most recently, Belle II measured the inclusive ratio $\frac{\mathrm{BR}(B \to Xe\nu)}{\mathrm{BR}(B \to X\mu\nu)} = 1.007 \pm 0.009 \pm 0.019$ [75] which also agrees with the SM prediction of $1.006 \pm 0.001$ [76]. The deviation from unity in the three ratios originates from phase space suppression due to the muon mass.

Although the charged current processes are well constrained, they do not provide competitive constraints. In our analysis we find that they are always subdominant compared to other rare $B$ meson decays $B \to K^{(\star)} + \mathrm{inv}$ and are thus not included in the discussion of Sect. 4. This can be understood from the different sizes of the SM contributions to the different processes: While charged current processes are induced at tree level in the SM via $W$ boson exchange, rare decays are only induced at loop level and are further suppressed by the Glashow–Iliopoulos–Maiani (GIM) mechanism. The new physics contributions from the operators in Eq. (1) are however of the same size for both charged-current and neutral-current processes. Finally, colliders may be used to search for new charged-current semi-leptonic operators, see e.g. [77,78], which results in constraints on the new physics scale in the $O(1 - 10)$ TeV range. Long-lived sterile neutrinos from meson decays may also be searched for at the proposed far-forward detectors at the (high-luminosity) LHC, SHiP and Belle II, see e.g. [79–81]. There are currently no constraints from leptonic $B_c$ decays.

## 4 Results

In the following we focus on the rare $B$ meson decay $B \to K^{(\star)} + \mathrm{inv}$ and present first an analysis with one operator being switched on at a time, which is followed by a discussion of correlations between pairs of operators.

In Fig. 2 we illustrate how a single operator may explain the observed decay $B^+ \to K^+ + \mathrm{inv}$ as a function of the sterile neutrino mass $m_1$. The light-blue band indicates the $1\sigma$-allowed region of parameter space which explains the simple weighted average for $\mathrm{BR}(B^+ \to K^+ + \mathrm{inv})$. The hatched light-blue region indicates the parameter space explaining the Belle II measurement. Wilson coefficients above the solid red and green contour lines are excluded at 90% CL by the non-observation of $B^0 \to K^{\star 0} + \mathrm{inv}$ and $B^0 \to K^0 + \mathrm{inv}$, respectively. The results do not depend on the neutrino flavour. In particular, the results are unchanged, when changing from first generation lepton doublets to second or third generation lepton doublets. We do not show plots for the scalar and tensor operators with a right-handed strange quark. They yield identical results as the operators with a left-handed strange quark, because the branching ratios are invariant under the exchange $s \leftrightarrow b$ for the LEFT scalar and tensor operators.

Figure 2 (bottom) clearly shows that tensor operators are not able to explain the observed excess in $B^+ \to K^+ + \mathrm{inv}$. The constraint from $B \to K^\star + \mathrm{inv}$ is weakened for large sterile neutrino masses $m_1 \sim 4$ GeV because of the larger mass of the $K^\star$ meson and thus reduced phase space. As large sterile neutrino masses modify the $q^2$ distribution and the experimental efficiency is generally lower for large $q^2$, a more careful analysis using the full $q^2$ distribution is required in this case. The result is independent of the lepton flavour and the same result applies to the tensor operator with right-handed strange quarks.

While vector operators $\mathcal{O}^{\mathrm{QN}}$ with massless sterile neutrinos are clearly excluded as explanation, Fig. 2 (top left) suggests the ability to explain the observed excess for sterile neutrino masses of $m_1 \gtrsim 1.5$ GeV. This feature is again due to the smaller phase space for decays to $K^\star$ mesons and
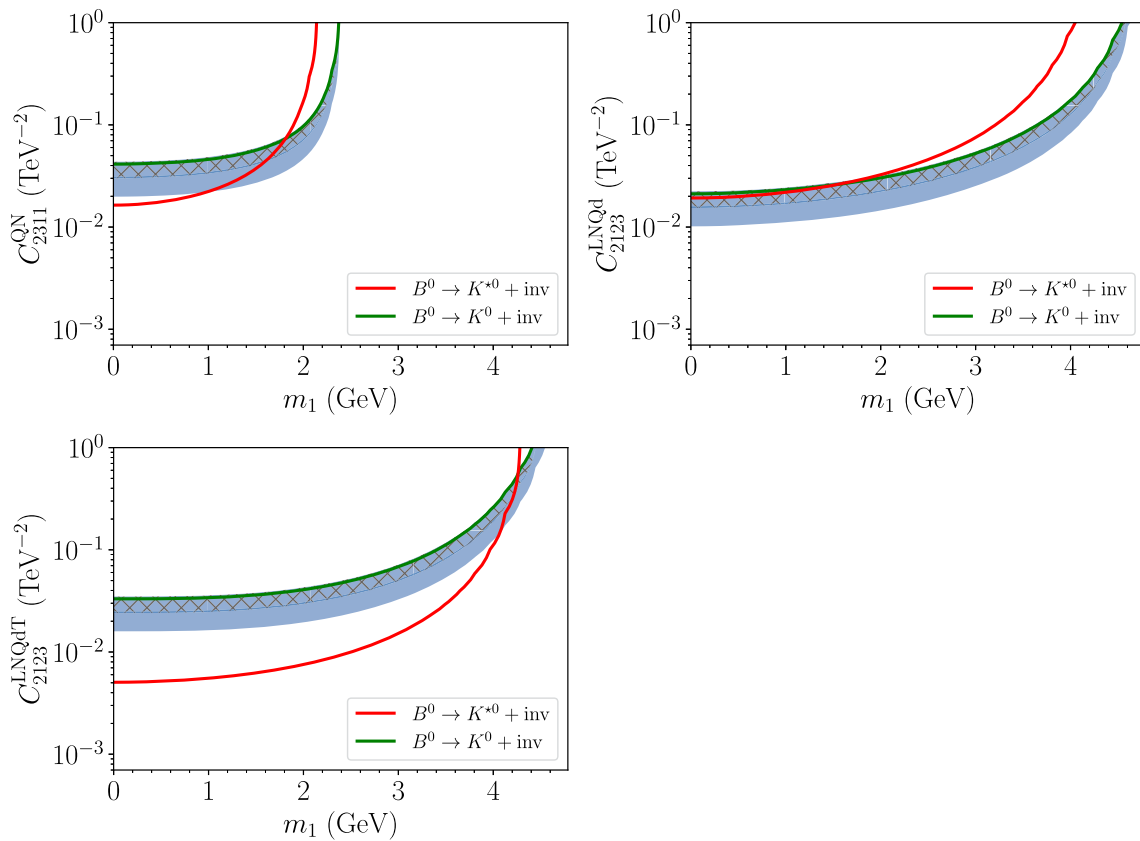
**Fig. 2** The red (green) contour line stands for the present bound on BR($B^0 \rightarrow K^{\star 0}(K^0)$ + inv), and the respective regions above these lines are therefore ruled out. The light-blue band symbolises the simple weighted average for BR($B^+ \rightarrow K^+$ + inv), and the hatched light-blue region is compatible with the 2023 Belle II measurement

requires a more detailed analysis using the $q^2$ distribution to arrive at a conclusive result. The same conclusion holds for the vector operator $\mathcal{O}^{\mathrm{dN}}$ with right-handed down-type quarks.

As shown in Fig. 2 (top right), the most promising explanation of the observed excess is provided by scalar operators $\mathcal{O}^{\mathrm{LNQd}}$ whose contribution to $B \rightarrow K^\star \nu \nu$ is suppressed. This opens up the possibility to explain the observed excess for the whole allowed sterile neutrino mass range. Note, although scalar operators with massless neutrinos do not have a sharp cutoff in the $q^2$ distribution, they dominantly contribute to the large $q^2$ region as illustrated in Fig. 1. As it has been pointed out in [7,45], the Belle II experiment is able to constrain them by searching for invisible $B_s$ decays which are currently unconstrained.

In the following we focus on scalar and vector operators which are most promising to explain the observed excess in $B^+ \rightarrow K^+$ + inv. Figure 3 shows the dependence of the (total) branching ratio BR($B^+ \rightarrow K^+ \nu \nu$) as a function of the Wilson coefficient for two benchmark masses of $m_1 = 0$ (1.5) GeV on the left (right). The vertical red (green) line indicates the most stringent constraint from $B \rightarrow K^\star$ + inv

($B \rightarrow K$ + inv), which excludes the region to the right of the line. The horizontal light-blue bands again indicate the region preferred by $B^+ \rightarrow K^+$ + inv. Figure 3 (top row) shows the branching ratio as a function of the Wilson coefficient for the vector operator $\mathcal{O}^{\mathrm{QN}}_{2311}$ with left-handed quark doublets. The top-left figure clearly illustrates the conflict between the measurement of $B^+ \rightarrow K^+$ + inv and the non-observation of $B^0 \rightarrow K^{\star 0}$ + inv for massless sterile neutrinos. For $m_1 = 1.5$ GeV, $B^0 \rightarrow K^{\star 0}$ + inv constrains $C^{\mathrm{QN}}_{2311} \leq 0.037 \, \mathrm{TeV}^{-2}$, which limits the excess in $B^+ \rightarrow K^+$ + inv to the region allowed by the simple weighted average, but precludes an explanation of the larger branching ratio measured by Belle II. The same result applies for the vector operator $\mathcal{O}^{\mathrm{dN}}$ with right-handed down-type quarks. Similarly, Fig. 3 (bottom row) illustrates the dependence of BR($B^+ \rightarrow K^+ \nu \nu$) on the scalar Wilson coefficient $C^{\mathrm{LNQd}}_{2123}$. The region to the left of the vertical green and red lines is consistent with the neutral decay modes $B^0 \rightarrow K^{\star 0} \nu \nu$ and thus the scalar operators are able to explain the observed excess.

In order to compare how future experimental results may impact the conclusions, we show in Fig. 4 the branching ratios for invisible $B_s$ decay (black), $B^0 \rightarrow K^{\star 0} \nu \nu$ (red), $B^+ \rightarrow$
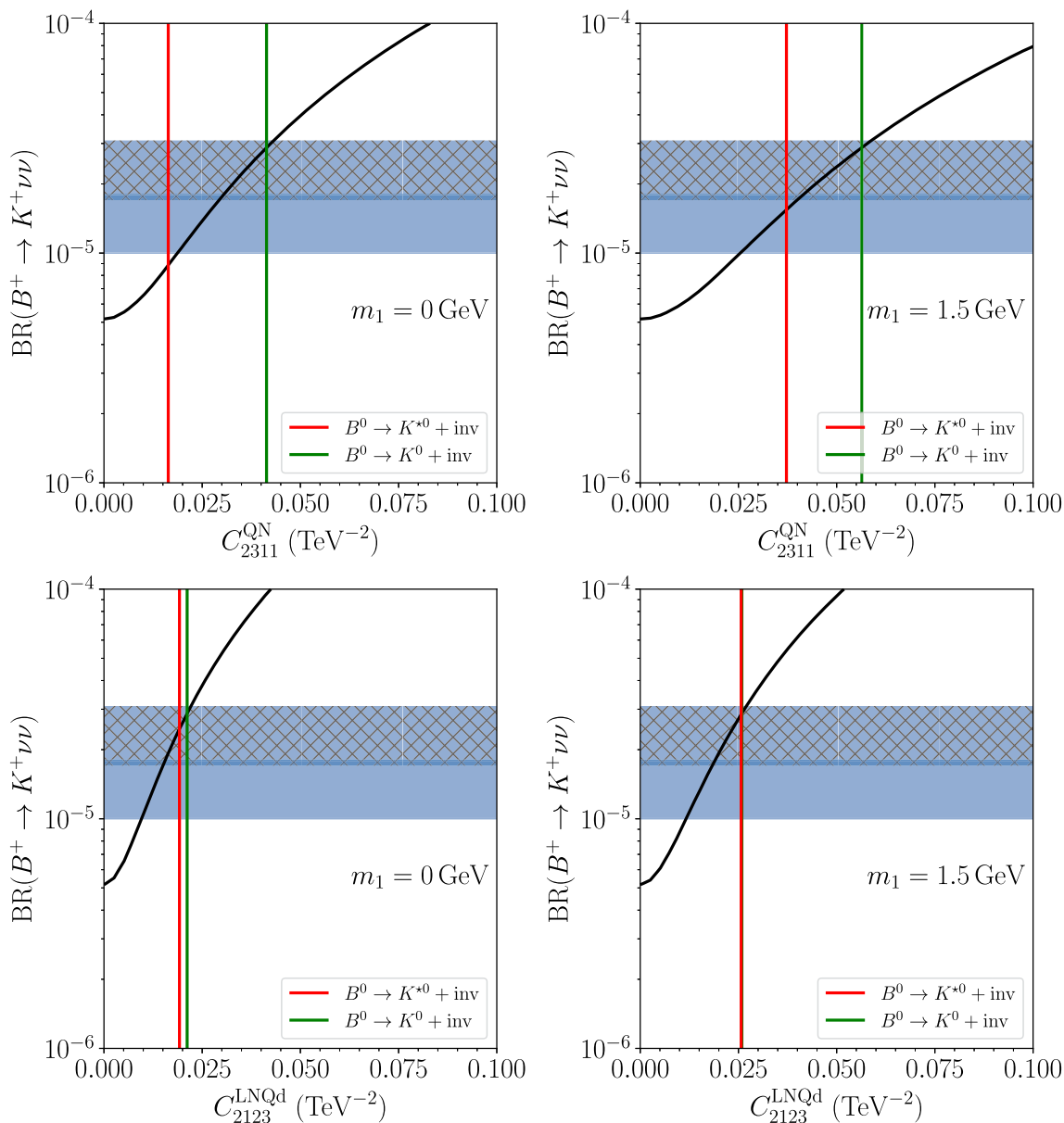
**Fig. 3** The red (green) line stands for the present bound on BR($B^0 \to K^{\star 0}(K^0) + \text{inv}$), and the respective regions to the right of these lines are therefore ruled out. The light-blue band symbolises the simple weighted average for BR($B^+ \to K^+ + \text{inv}$), and the hatched light-blue region is compatible with the 2023 Belle II measurement. The plots in the top row also apply to the operator $\mathcal{O}^{\text{dN}}$ and the plots in the bottom row also apply to $\mathcal{O}_{2132}^{\text{LNQd}}$

$K^{\star +}\nu\nu$ (orange), $B^0 \to K^0\nu\nu$ (green), and $B^+ \to K^+\nu\nu$ (blue) as a function of the scalar $C_{2123}^{\text{LNQd}}$ and vector $C_{2311}^{\text{QN}}$ Wilson coefficient as solid lines and the current upper limits as dashed lines. The region to the right of the intersection of the dashed and solid lines of the same colour is already excluded. The branching ratios of the charged and neutral $B$ meson decay channels are approximately equal due to isospin symmetry. Belle II provided a detailed study of future sensitivities in [82]: In particular with an integrated luminosity of 1 ab$^{-1}$, Belle II is sensitive to the signal strength of 2.06 for

$B^0 \to K^0 + \text{inv}$ and thus is able to probe the entire region favoured by $B^+ \to K^+ + \text{inv}$. An improved analysis may even reach a signal strength of 1.37. Similarly, the expected sensitivities for the decays $B \to K^\star + \text{inv}$ are 1.08(0.72) and 2.04(1.45) for the neutral and charged $B$ meson decays, where we indicated the expected improved sensitivities in parentheses. Hence, also the searches for $B^0 \to K^{\star 0} + \text{inv}$ are able to probe most of the preferred parameter space for scalar operators, while $B^+ \to K^{\star +} + \text{inv}$ is less sensitive. For the vector operator explanation, the decays $B \to K^\star\nu\nu$ are
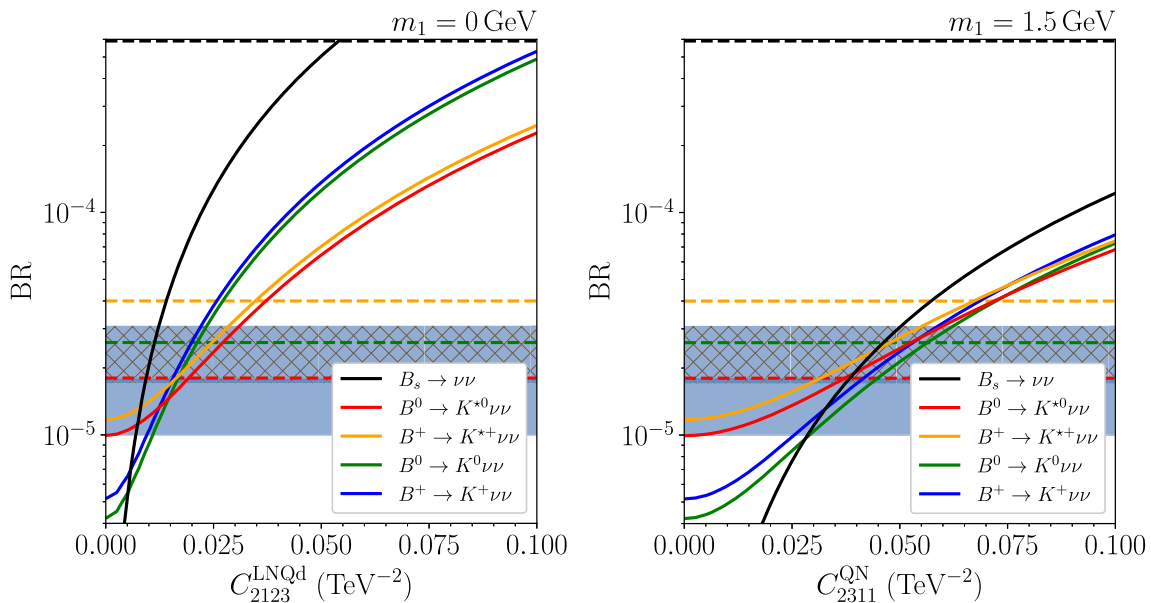
**Fig. 4** Branching ratios of several decay modes as a function of the scalar (left) and vector (right) Wilson coefficients for fixed sterile neutrino mass. The dashed horizontal contours indicate the current upper bounds for $B^0 \to K^{\star 0} + \text{inv}$ (red), $B^+ \to K^{\star +} + \text{inv}$ (orange),
$B^0 \to K^0 + \text{inv}$ (green), and $B_s \to \text{inv}$ (black). The light-blue band symbolises the simple weighted average for $\text{BR}(B^+ \to K^+ + \text{inv})$ and the hatched light-blue region is compatible with the 2023 Belle II measurement

not expected to be sensitive to the whole preferred parameter space.

There is currently only a weak upper limit on the branching ratio of invisible $B_s$ decays based on LEP data [65]. Belle II's ability to probe $\text{BR}(B_s \to \text{inv}) \gtrsim 1.1 \times 10^{-5}$ with an integrated luminosity of 5 ab$^{-1}$ [66] will provide a conclusive test of the described explanations of $B^+ \to K^+ \nu\nu$ for both scalar and vector operators. The scalar operator contribution is not helicity suppressed, as outlined in Sect. 3, and thus the invisible $B_s$ decay is sensitive to the full sterile neutrino mass range. The vector operator contribution is helicity suppressed, but the explanation of the excess in $B^+ \to K^+ + \text{inv}$ requires large sterile neutrino masses $m_1 \gtrsim 1.5$ GeV and thus invisible $B_s$ decays are also able to probe the vector operator scenario.

We finally turn our attention to correlations between different operators. In Fig. 5, we present the 90% CL exclusion contours for $B^0 \to K^{\star 0} + \text{inv}$ ($B^0 \to K^0 + \text{inv}$) in red (green) using the current upper limits [3,4]. Larger Wilson coefficients are excluded. The constraint from $B^+ \to K^{\star +} + \text{inv}$ is weaker than $B^0 \to K^{\star 0} + \text{inv}$ and thus not shown for clarity. Similar to above, the blue-shaded region indicates the simple weighted average for $\text{BR}(B^+ \to K^+ + \text{inv})$ and the hatched region the 2023 Belle II measurement of $B^+ \to K^+ + \text{inv}$.

Figure 5 (top row) illustrates the correlation between the vector operators with right-handed down-type quarks, $\mathcal{O}_{2311}^{\text{dN}}$, and left-handed quark doublets, $\mathcal{O}_{2311}^{\text{QN}}$. Their contribution to the branching ratio of $B \to K\nu\nu$ is proportional to $\left| C_{2311}^{\text{QN}} + C_{2311}^{\text{dN}} \right|^2$, while for the branching ratios of $B \to K^{\star}\nu\nu$ there are two independent contributions proportional to the square of the sum and difference of the two Wilson coefficients. This explains the shape of the contour lines: While the non-observation of $B \to K^{\star} + \text{inv}$ results in an elliptical exclusion region, the decay $B \to K\nu\nu$ is insensitive to $C_{2311}^{\text{QN}} = -C_{2311}^{\text{dN}}$ and thus the search for $B \to K + \text{inv}$ is unable to probe this direction in parameter space. Increasing the sterile neutrino mass to $m_1 = 1.5$ GeV, see Fig. 5 (top right), reduces the contribution to $B \to K^{\star}\nu\nu$ and thus weakens the $B \to K^{\star} + \text{inv}$ constraint. Consequently, the allowed region inside the red ellipse widens.

The plots in Fig. 5 (bottom row) show the correlation between the scalar operator $\mathcal{O}_{2123}^{\text{LNQd}}$ and the vector operator $\mathcal{O}_{2311}^{\text{QN}}$ with left-handed quark doublets. The elliptical exclusion regions are due to the absence of complete cancellations between the two operators. In fact, there is no interference between the two operators in the massless limit. The bottom-left plot clearly shows the preference for the pure scalar operator scenario for massless sterile neutrinos. For massive sterile neutrinos, the constraint from $B \to K^{\star} + \text{inv}$ weakens. The bottom-right plot shows the case with $m_1 = 1.5$ GeV, where the dominant constraint originates from $B^0 \to K^{\star 0} + \text{inv}$ and the constraint from $B \to K^0 + \text{inv}$ is subdominant. The same conclusions holds, if the quark flavours of the scalar operator are exchanged, $s \leftrightarrow b$, or if the vector operator $\mathcal{O}^{\text{dN}}$ with right-handed down-type quarks is considered.
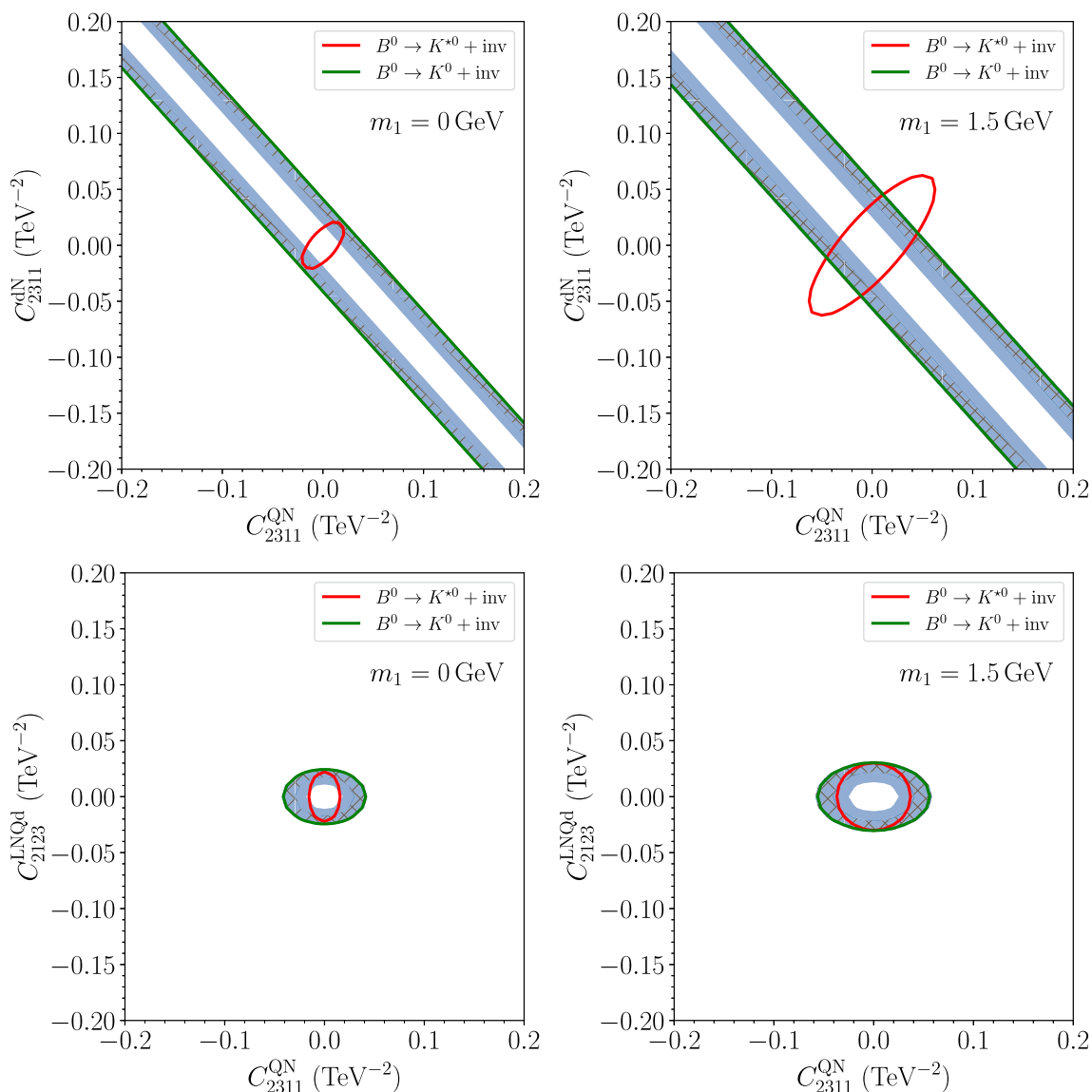
**Fig. 5** The red (green) contour line stands for the present bound on BR($B^0 \to K^{\star 0}(K^0)$ + inv), and the respective regions outside of these lines are therefore ruled out. The light-blue band symbolises the simple weighted average for BR($B^+ \to K^+$ + inv), and the hatched light-blue region is compatible with the 2023 Belle II measurement

## 5 UV completions

We briefly outline possible UV completions for the scalar and vector operators discussed in the previous section, see [83] for a detailed discussion of tree-level UV completions of dimension-6 operators in $\nu$SMEFT. The most straightforward UV completion of the scalar operator $\mathcal{O}^{\text{LNQd}}$ is provided by a second electroweak doublet scalar $\eta \sim (\mathbf{1}, \mathbf{2}, -\frac{1}{2})$ with its Yukawa interactions $\bar{L}N\eta$ and $\bar{Q}i\sigma_2\eta^*d$. Integrating out the electroweak doublet scalar $\eta$ results in the scalar operator $\mathcal{O}^{\text{LNQd}}$, but it also generates the 4-fermion operators $(\bar{L}\gamma_\mu L)(\bar{N}\gamma^\mu N)$ and $(\bar{Q}\gamma_\mu Q)(\bar{d}\gamma_\mu d)$. The latter contributes to $B_s - \overline{B_s}$ mixing and the former to charged lepton

decays $\ell_i \to \ell_j$ + inv which both have to be considered in a UV-complete model. The required size of the scalar Wilson coefficient $C^{\text{LNQd}} \sim 0.02\,\text{TeV}^{-2}$ requires the electroweak doublet scalar to have a mass of at most $\mathcal{O}(7)$ TeV for Yukawa couplings of order unity.

The vector operators are straightforwardly generated using leptoquarks, see e.g. [84] for a review. The $S_1 \sim (\bar{\mathbf{3}}, \mathbf{1}, \frac{1}{3})$ leptoquark leads to the operator $\mathcal{O}^{\text{dN}}$ via its Yukawa interaction $\overline{N^c}S_1d$ and thus does not contribute to $B_s - \overline{B_s}$ mixing at tree level. Its other leptoquark couplings generate the SMEFT operators $\mathcal{O}^{\text{eu}}$, and $\mathcal{O}^{\text{LeQu}(1,3)}$, and $\mathcal{O}^{\text{LQ}(1,3)}$, see e.g. [85]. Similarly, the leptoquark $\tilde{R}_2 \sim (\mathbf{3}, \mathbf{2}, \frac{1}{6})$ may gen-

erate the operator $\mathcal{O}^{\mathrm{QN}}$ via its Yukawa interaction $\overline{Q}\tilde{R}_2 N$, which does not contribute to $B_s - \overline{B_s}$ mixing at tree level. Its other Yukawa interaction $\bar{d}\tilde{R}_2 L$ contributes to the SMEFT operator $\mathcal{O}^{\mathrm{Ld}}$ [85]. The required size of the vector Wilson coefficient $C^{\mathrm{QN,dN}} \sim 0.03\,\mathrm{TeV}^{-2}$ requires the leptoquark to have a mass of at most $\mathcal{O}(6)$ TeV for Yukawa couplings of order unity. The operators $\mathcal{O}^{\mathrm{LQ(1,3)}}$ and $\mathcal{O}^{\mathrm{Ld}}$ may also contribute to $B \to K^{(\star)}\nu\nu$, but they are strongly constrained by searches for $B \to K^{(\star)}\ell\bar{\ell}$ for light charged leptons $\ell$, see e.g. [7,45].

## 6 Conclusions

We studied how the recently observed excess in $B^+ \to K^+ +$ inv may be explained within $\nu$SMEFT. Within $\nu$SMEFT there are four 4-fermion operators with sterile neutrinos which may contribute to $B^+ \to K^+ +$ inv: two vector, one scalar and one tensor operator. We would like to stress that massive sterile neutrinos and scalar and tensor operators modify the $q^2$ distribution with respect to the SM prediction based on massless neutrinos contributing via a vector operator. The present analysis is entirely based on the branching ratios and we only comment on the $q^2$ distribution, because it is currently not available. The tensor operator is strongly constrained by $B^0 \to K^{\star 0} +$ inv and thus is not able to significantly contribute to $B^+ \to K^+ +$ inv.

We find that the excess in $B^+ \to K^+ +$inv is most straightforwardly explained by scalar operators with sterile neutrinos irrespective of their mass. This scenario can be conclusively probed using invisible $B_s$ decays at Belle II and the rare semileptonic decay $B^0 \to K^{(\star)0} +$ inv in the near future using $1\,\mathrm{ab}^{-1}$ of data. Vector operators may be able to explain the excess of $B^+ \to K^+ +$ inv for intermediate sterile neutrino masses of $m_1 \gtrsim 1.5$ GeV assuming no significant changes to the $q^2$ distribution. While $B \to K^\star +$ inv strongly constrains this possibility for light sterile neutrinos, the decay $B \to K^\star +$ inv is less sensitive for sterile neutrino masses $m_1 \sim 1.5$ GeV due to phase space suppression, but still provides a constraint. Most of the parameter space of this solution can similarly be probed with the invisible $B_s$ decay and $B^0 \to K^{(\star)0} +$ inv.

We finally outline tree-level UV completions for the scalar and vector operators. The scalar operator may be generated using an electroweak doublet scalar, which however also contributes to $B_s - \overline{B_s}$ mixing at tree level. The vector operators can be straightforwardly generated using leptoquarks: the $S_1$ leptoquark may result in $\mathcal{O}^{\mathrm{dN}}$ and the $\tilde{R}_2$ leptoquark in $\mathcal{O}^{\mathrm{QN}}$. Generally, all UV completions also generate other $\nu$SMEFT operators, but for the two leptoquarks it is in principle possible to avoid them. It however requires to set all other Yukawa couplings to zero, which may be considered unnatural. This motivates to consider the full set of relevant $\nu$SMEFT operators in a future study and to investigate explanations of the excess in UV complete models together with other observables.

**Data Availability Statement** This manuscript has no associated data or the data will not be deposited. [Authors' comment: All figures in the paper can be reproduced with the analytical results provided in the article together with publicly available data and results which have been referenced.]

## A $S, P, V, A, \mathcal{T}$ basis

For the calculation it is convenient to employ a basis with well-defined parity properties which has been used in [46]. In this appendix we provide the matching of the chiral LEFT basis used in the main part of the text to this basis both for charged current operators with Dirac fermions and neutral current neutrino-quark operators with Majorana fermions.

A.1 Charged current operators with Dirac fermions

We define the operator basis as

$$\mathcal{L} = c_H \sum_i \sum_{\alpha,\beta} (C_{i,\alpha\beta} O_{i,\alpha\beta} + C'_{i,\alpha\beta} O'_{i,\alpha\beta}), \tag{17}$$

where $i$ runs over $S, P, V, A, \mathcal{T}$ and $c_H$ determines the normalisation of the operators. Similar to [12] we use $c_H = 1$, which differs from [46] where the normalisation $c_H = \frac{4G_F}{\sqrt{2}}\frac{\alpha}{4\pi} V_{ts}^* V_{tb}$ has been used. The operators are

$$O_{S(P)\alpha\beta} = (\overline{c_L}b)(\overline{e_\alpha}(\gamma_5)\nu_\beta),$$
$$O_{V(A)\alpha\beta} = (\overline{c_L}\gamma^\mu b)(\overline{e_\alpha}\gamma_\mu(\gamma_5)\nu_\beta), \tag{18}$$
$$O_{\mathcal{T}\alpha\beta} = (\overline{c_L}\sigma^{\mu\nu}b)(\overline{e_\alpha}\sigma_{\mu\nu}\nu_\beta).$$

The primed operators are obtained by replacing $c_L \rightarrow c_R$, i.e. $\mathcal{O}' = \mathcal{O}|_{c_L \rightarrow c_R}$ where $q_{L,R} \equiv P_{L,R}q$. The Wilson coefficients in the $S, P, V, A, \mathcal{T}$ basis are given in terms of the chiral basis by

$$
C_{V\alpha\beta} = \frac{1}{2}\left(C^{\mathrm{VRL*}}_{vedu,\beta abc} + C^{\mathrm{VLL*}}_{vedu,\beta abc}\right),
$$

$$
C_{A\alpha\beta} = \frac{1}{2}\left(C^{\mathrm{VRL*}}_{vedu,\beta abc} - C^{\mathrm{VLL*}}_{vedu,\beta abc}\right),
$$

$$
C'_{V\alpha\beta} = \frac{1}{2}\left(C^{\mathrm{VRR*}}_{vedu,\beta abc} + C^{\mathrm{VLR*}}_{vedu,\beta abc}\right),
$$

$$
C'_{A\alpha\beta} = \frac{1}{2}\left(C^{\mathrm{VRR*}}_{vedu,\beta abc} - C^{\mathrm{VLR*}}_{vedu,\beta abc}\right),
$$

$$
C_{S\alpha\beta} = \frac{1}{2}\left(C^{\mathrm{SLL*}}_{vedu,\beta abc} + C^{\mathrm{SRL*}}_{vedu,\beta abc}\right), \qquad (19)
$$

$$
C_{P\alpha\beta} = \frac{1}{2}\left(C^{\mathrm{SLL*}}_{vedu,\beta abc} - C^{\mathrm{SRL*}}_{vedu,\beta abc}\right),
$$

$$
C'_{S\alpha\beta} = \frac{1}{2}\left(C^{\mathrm{SLR*}}_{vedu,\beta abc} + C^{\mathrm{SRR*}}_{vedu,\beta abc}\right),
$$

$$
C'_{P\alpha\beta} = \frac{1}{2}\left(C^{\mathrm{SLR*}}_{vedu,\beta abc} - C^{\mathrm{SRR*}}_{vedu,\beta abc}\right),
$$

$$
C_{T\alpha\beta} = C^{\mathrm{TLL*}}_{vedu,\beta abc},
$$

$$
C'_{T\alpha\beta} = C^{\mathrm{TRR*}}_{vedu,\beta abc}.
$$

### A.2 Neutral current neutrino-quark operators with Majorana neutrinos

Following [12] we define the leptonic helicity amplitudes for Majorana spinors with an additional factor of $1/2$ in the effective Lagrangian, such that the leptonic helicity amplitudes have the same form as for Dirac fermions. The effective Lagrangian is thus given by

$$
\mathcal{L} = \frac{1}{2}c_H \sum_i \sum_{\alpha,\beta} (C_{i,\alpha\beta}O_{i,\alpha\beta} + C'_{i,\alpha\beta}O'_{i,\alpha\beta}). \qquad (20)
$$

The operators with Majorana neutrinos are obtained from Eq. (18) using $e_\alpha \rightarrow \nu_\alpha$ and $c \rightarrow s$. The operators have well-defined symmetry properties: the (pseudo-)scalar and axial-vector operators are symmetric in the neutrino flavour indices and the vector and tensor operators are antisymmetric. We find for the Wilson coefficients using the $S, P, V, A, \mathcal{T}$ basis

$$
C_{V\alpha\beta} = C^{\mathrm{VLL}}_{vd,[\alpha\beta]sb},
$$

$$
C_{A\alpha\beta} = -C^{\mathrm{VLL}}_{vd,(\alpha\beta)sb},
$$

$$
C'_{V\alpha\beta} = C^{\mathrm{VLR}}_{vd,[\alpha\beta]sb},
$$

$$
C'_{A\alpha\beta} = -C^{\mathrm{VLR}}_{vd,(\alpha\beta)sb},
$$

$$
C_{S\alpha\beta} = C^{\mathrm{SLR}}_{vd,(\alpha\beta)sb} + C^{\mathrm{SLL*}}_{vd,(\beta\alpha)bs},
$$

$$
C_{P\alpha\beta} = -C^{\mathrm{SLR}}_{vd,(\alpha\beta)sb} + C^{\mathrm{SLL*}}_{vd,(\beta\alpha)bs},
$$

$$
C'_{S\alpha\beta} = C^{\mathrm{SLL}}_{vd,(\alpha\beta)sb} + C^{\mathrm{SLR*}}_{vd,(\beta\alpha)bs},
$$

$$
C'_{P\alpha\beta} = -C^{\mathrm{SLL}}_{vd,(\alpha\beta)sb} + C^{\mathrm{SLR*}}_{vd,(\beta\alpha)bs},
$$

$$
C_{T\alpha\beta} = 2C^{\mathrm{TLL}}_{vd,[\beta\alpha]bs},
$$

$$
C'_{T\alpha\beta} = 2C^{\mathrm{TLL}}_{vd,[\alpha\beta]sb}, \qquad (21)
$$

where $\alpha, \beta$ denote the neutrino flavours. Parentheses (…) indicate symmetrisation and square brackets […] indicate anti-symmetrisation of the neutrino flavour indices as in

$$
M_{(ab)} \equiv \frac{1}{2}\left(M_{ab} + M_{ba}\right), \qquad M_{[ab]} \equiv \frac{1}{2}\left(M_{ab} - M_{ba}\right). \qquad (22)
$$

### B $B_s \rightarrow \nu\nu$

An important observable is given by invisible $B_s$ decays. In this section, we provide the general branching ratio for $B_s \rightarrow \nu_\alpha \nu_\beta$. We define the form factors

$$
\langle 0|\bar{s}\gamma^\mu\gamma_5 b|\bar{B}_s(P)\rangle = if_{B_s}P^\mu,
$$

$$
\langle 0|\bar{s}\gamma_5 b|\bar{B}_s(P)\rangle = -i\frac{h_{B_s}}{m_b + m_s}, \qquad (23)
$$

where the scalar and vector form factors are related by $h_{B_s} = m^2_{B_s}f_{B_s}$. Using the $S, P, V, A, \mathcal{T}$ basis, we find for the branching ratio of $B_s \rightarrow \nu_\alpha \nu_\beta$

$$
\mathrm{BR}(B_s \rightarrow \nu_\alpha\nu_\beta) = \frac{\lambda^{1/2}(1, x^2_\alpha, x^2_\beta)\tau_{B_s}m^3_{B_s}f^2_{B_s}}{64\pi(1 + \delta_{\alpha\beta})}
$$

$$
\times \Bigg(\left|C_{V\alpha\beta} - C'_{V\alpha\beta}\right|^2 (1 - (x_\alpha + x_\beta)^2)(x_\alpha - x_\beta)^2
$$

$$
+ \left|C_{A\alpha\beta} - C'_{A\alpha\beta}\right|^2 (1 - (x_\alpha - x_\beta)^2)(x_\alpha + x_\beta)^2
$$

$$
+ \left|C_{S\alpha\beta} - C'_{S\alpha\beta}\right|^2 \frac{1 - (x_\alpha + x_\beta)^2}{(x_b + x_s)^2}
$$

$$
+ \left|C_{P\alpha\beta} - C'_{P\alpha\beta}\right|^2 \frac{1 - (x_\alpha - x_\beta)^2}{(x_b + x_s)^2}
$$

$$
+ 2\,\mathrm{Re}\left[(C_{V\alpha\beta} - C'_{V\alpha\beta})(C_{S\alpha\beta} - C'_{S\alpha\beta})^*\right]
$$

$$
\times \frac{x_\alpha(1 - x_\alpha x_\beta - x^2_\alpha) - x_\beta(1 - x_\alpha x_\beta - x^2_\beta)}{x_b + x_s}
$$

$$
+ 2\,\mathrm{Re}\left[(C_{A\alpha\beta} - C'_{A\alpha\beta})(C_{P\alpha\beta} - C'_{P\alpha\beta})^*\right]
$$

$$
\times \frac{x_\alpha(1 + x_\alpha x_\beta - x^2_\alpha) + x_\beta(1 + x_\alpha x_\beta - x^2_\beta)}{x_b + x_s}\Bigg), \qquad (24)
$$

with $x_\alpha = \frac{m_\alpha}{m_{B_s}}$ and the Källén function $\lambda(x, y, z) \equiv x^2 + y^2 + z^2 - 2xy - 2xz - 2yz$. There is no interference between the operators with different neutrino exchange symmetry and there is no contribution from tensor operators. The branching

ratio is symmetric in the final state neutrino flavours. For identical final state neutrinos the branching ratio reduces to

$$
\begin{aligned}
\mathrm{BR}(B_s \to \nu_\alpha \nu_\alpha) = {} & \frac{\tau_{B_s} m_{B_s}^3 f_{B_s}^2}{128\pi} \\
& \times \Bigg( 4 \left| C_{A\alpha\alpha} - C'_{A\alpha\alpha} \right|^2 x_\alpha^2 \sqrt{1 - 4x_\alpha^2} \\
& + \left| C_{S\alpha\alpha} - C'_{S\alpha\alpha} \right|^2 \frac{(1 - 4x_\alpha^2)^{3/2}}{x_b^2} \\
& + \left| C_{P\alpha\alpha} - C'_{P\alpha\alpha} \right|^2 \frac{\sqrt{1 - 4x_\alpha^2}}{x_b^2} \\
& + 4 \, \mathrm{Re} \left[ (C_{A\alpha\alpha} - C'_{A\alpha\alpha})(C_{P\alpha\alpha} - C'_{P\alpha\alpha})^* \right] \\
& \times \frac{x_\alpha \sqrt{1 - 4x_\alpha^2}}{x_b} \Bigg),
\end{aligned}
\tag{25}
$$

where we used $x_s \ll x_b$.

## References

1. Belle II Collaboration, A. Glazov, News from Belle II. EPS conference (2023)
2. D. Bečirević, G. Piazza, O. Sumensari, Revisiting $B \to K^{(*)}\nu\bar{\nu}$ decays in the Standard Model and beyond. Eur. Phys. J. C **83**(3), 252 (2023). https://doi.org/10.1140/epjc/s10052-023-11388-z. arXiv:2301.06990 [hep-ph]
3. Belle Collaboration, O. Lutz et al., Search for $B \to h^{(*)}\nu\bar{\nu}$ with the full Belle $\Upsilon(4S)$ data sample. Phys. Rev. D **87**(11), 111103 (2013). https://doi.org/10.1103/PhysRevD.87.111103. arXiv:1303.3719 [hep-ex]
4. Belle Collaboration, J. Grygier et al., Search for $B \to h\nu\bar{\nu}$ decays with semileptonic tagging at Belle. Phys. Rev. D **96**(9), 091101 (2017). https://doi.org/10.1103/PhysRevD.96.091101. arXiv:1702.03224 [hep-ex] [Addendum: Phys. Rev. D 97, 099902 (2018)]
5. BaBar Collaboration, J.P. Lees et al., Search for $B \to K^{(*)}\nu\bar{\nu}$ and invisible quarkonium decays. Phys. Rev. D **87**(11), 112005 (2013). https://doi.org/10.1103/PhysRevD.87.112005. arXiv:1303.7465 [hep-ex]
6. Belle-II Collaboration, F. Abudinén et al., Search for $B+ \to K + \nu\bar{\nu}$ decays using an inclusive tagging method at Belle II. Phys. Rev. Lett. **127**(18), 181802 (2021). https://doi.org/10.1103/PhysRevLett.127.181802. arXiv:2104.12624 [hep-ex]
7. R. Bause, H. Gisbert, G. Hiller, Implications of an enhanced $B \to K\nu\bar{\nu}$ branching ratio. arXiv:2309.00075 [hep-ph]
8. L. Allwicher, D. Becirevic, G. Piazza, S. Rosauro-Alcaraz, O. Sumensari, Understanding the first measurement of $\mathcal{B}(B \to K\nu\bar{\nu})$. arXiv:2309.02246 [hep-ph]
9. P. Athron, R. Martinez, C. Sierra, $B$ meson anomalies and large $B^+ \to K^+\nu\bar{\nu}$ in non-universal $U(1)'$ models. arXiv:2308.13426 [hep-ph]
10. T.E. Browder, N.G. Deshpande, R. Mandal, R. Sinha, Impact of $B \to K\nu\bar{\nu}$ measurements on beyond the Standard Model theories. Phys. Rev. D **104**(5), 053007 (2021). https://doi.org/10.1103/PhysRevD.104.053007. arXiv:2107.01080 [hep-ph]
11. X.G. He, G. Valencia, $RK(*)\nu$ and non-standard neutrino interactions. Phys. Lett. B **821**, 136607 (2021). https://doi.org/10.1016/j.physletb.2021.136607. arXiv:2108.05033 [hep-ph]
12. T. Felkl, S.L. Li, M.A. Schmidt, A tale of invisibility: constraints on new physics in $b \to s\nu\nu$. JHEP **12**, 118 (2021). https://doi.org/10.1007/JHEP12(2021)118. arXiv:2111.04327 [hep-ph]
13. X.-G. He, X.-D. Ma, G. Valencia, FCNC B and K meson decays with light bosonic Dark Matter. JHEP **03**, 037 (2023). https://doi.org/10.1007/JHEP03(2023)037. arXiv:2209.05223 [hep-ph]
14. M. Ovchynnikov, M.A. Schmidt, T. Schwetz, Complementarity of $B \to K^{(*)}\mu\bar{\mu}$ and $B \to K^{(*)} +$ inv for searches of GeV-scale Higgs-like scalars. Eur. Phys. J. C **83**(9), 791 (2023). https://doi.org/10.1140/epjc/s10052-023-11975-0. arXiv:2306.09508 [hep-ph]
15. P. Asadi, A. Bhattacharya, K. Fraser, S. Homiller, A. Parikh, Wrinkles in the Froggatt–Nielsen mechanism and flavorful new physics. JHEP **10**, 069 (2023). https://doi.org/10.1007/JHEP10(2023)069. arXiv:2308.01340 [hep-ph]
16. C. Bird, P. Jackson, R.V. Kowalewski, M. Pospelov, Search for dark matter in $b \to s$ transitions with missing energy. Phys. Rev. Lett. **93**, 201803 (2004). https://doi.org/10.1103/PhysRevLett.93.201803. arXiv:hep-ph/0401195
17. W. Altmannshofer, A.J. Buras, D.M. Straub, M. Wick, New strategies for New Physics search in $B \to K^*\nu\bar{\nu}$, $B \to K\nu\bar{\nu}$ and $B \to X_s\nu\bar{\nu}$ decays. JHEP **04**, 022 (2009). https://doi.org/10.1088/1126-6708/2009/04/022. arXiv:0902.0160 [hep-ph]
18. Z.G. Berezhiani, M.Y. Khlopov, R.R. Khomeriki, On the possible test of quantum flavor dynamics in the searches for rare decays of heavy particles. Sov. J. Nucl. Phys. **52**, 344–347 (1990)
19. Z.G. Berezhiani, M.Y. Khlopov, Physical and astrophysical consequences of breaking of the symmetry of families (in Russian). Sov. J. Nucl. Phys. **51**, 935–942 (1990)
20. Z.G. Berezhiani, M.Y. Khlopov, The theory of broken gauge symmetry of families (in Russian). Sov. J. Nucl. Phys. **51**, 739–746 (1990)
21. A. Filimonova, R. Schäfer, S. Westhoff, Probing dark sectors with long-lived particles at BELLE II. Phys. Rev. D **101**(9), 095006 (2020). https://doi.org/10.1103/PhysRevD.101.095006. arXiv:1911.03490 [hep-ph]
22. T. Ferber, A. Filimonova, R. Schäfer, S. Westhoff, Displaced or invisible? ALPs from B decays at Belle II. JHEP **04**, 131 (2023). https://doi.org/10.1007/JHEP04(2023)131. arXiv:2201.06580 [hep-ph]
23. S. Iguro, Y. Omura, Status of the semileptonic $B$ decays and muon g-2 in general 2HDMs with right-handed neutrinos. JHEP **05**, 173 (2018). https://doi.org/10.1007/JHEP05(2018)173. arXiv:1802.01732 [hep-ph]
24. A. Azatov, D. Barducci, D. Ghosh, D. Marzocca, L. Ubaldi, Combined explanations of B-physics anomalies: the sterile neutrino solution. JHEP **10**, 092 (2018). https://doi.org/10.1007/JHEP10(2018)092. arXiv:1807.10745 [hep-ph]
25. P. Asadi, M.R. Buckley, D. Shih, Asymmetry observables and the origin of $R_{D^{(*)}}$ anomalies. Phys. Rev. D **99**(3), 035015 (2019). https://doi.org/10.1103/PhysRevD.99.035015. arXiv:1810.06597 [hep-ph]
26. K.S. Babu, B. Dutta, R.N. Mohapatra, A theory of R(D*, D) anomaly with right-handed currents. JHEP **01**, 168 (2019). https://doi.org/10.1007/JHEP01(2019)168. arXiv:1811.04496 [hep-ph]
27. J. Heeck, D. Teresi, Pati–Salam explanations of the B-meson anomalies. JHEP **12**, 103 (2018). https://doi.org/10.1007/JHEP12(2018)103. arXiv:1808.07492 [hep-ph]
28. J.D. Gómez, N. Quintero, E. Rojas, Charged current $b \to c\tau\bar{\nu}_\tau$ anomalies in a general $W'$ boson scenario. Phys. Rev. D **100**(9), 093003 (2019). https://doi.org/10.1103/PhysRevD.100.093003. arXiv:1907.08357 [hep-ph]
29. Z. Ligeti, M. Papucci, D.J. Robinson, New physics in the visible final states of $B \to D^{(*)}\tau\nu$. JHEP **01**, 083 (2017). https://doi.org/10.1007/JHEP01(2017)083. arXiv:1610.02045 [hep-ph]

30. D.J. Robinson, B. Shakya, J. Zupan, Right-handed neutrinos and $R(D^{(*)})$. JHEP **02**, 119 (2019). https://doi.org/10.1007/JHEP02(2019)119. arXiv:1807.04753 [hep-ph]

31. D. Bardhan, D. Ghosh, $B$-meson charged current anomalies: the post-Moriond 2019 status. Phys. Rev. D **100**(1), 011701 (2019). https://doi.org/10.1103/PhysRevD.100.011701. arXiv:1904.10432 [hep-ph]

32. S. Balaji, M.A. Schmidt, Unified SU(4) theory for the $R_{D(*)}$ and $R_{K(*)}$ anomalies. Phys. Rev. D **101**(1), 015026 (2020). https://doi.org/10.1103/PhysRevD.101.015026. arXiv:1911.08873 [hep-ph]

33. R. Mandal, C. Murgui, A. Peñuelas, A. Pich, The role of right-handed neutrinos in $b \rightarrow c\tau\bar{\nu}$ anomalies. JHEP **08**(08), 022 (2020). https://doi.org/10.1007/JHEP08(2020)022. arXiv:2004.06726 [hep-ph]

34. M.-L. Du, N. Penalva, E. Hernández, J. Nieves, New physics effects on $\Lambda_b \rightarrow \Lambda_c^* \tau \bar{\nu}_\tau$ decays. Phys. Rev. D **106**(5), 055039 (2022). https://doi.org/10.1103/PhysRevD.106.055039. arXiv:2207.10529 [hep-ph]

35. A. Datta, H. Liu, D. Marfatia, $B \rightarrow D(*)\ell X$ decays in effective field theory with massive right-handed neutrinos. Phys. Rev. D **106**(1), L011702 (2022). https://doi.org/10.1103/PhysRevD.106.L011702. arXiv:2204.01818 [hep-ph]

36. P. Minkowski, $\mu \rightarrow e\gamma$ at a Rate of One Out of $10^9$ muon decays? Phys. Lett. B **67**, 421–428 (1977). https://doi.org/10.1016/0370-2693(77)90435-X

37. T. Asaka, M. Shaposhnikov, The $\nu$MSM, dark matter and baryon asymmetry of the universe. Phys. Lett. B **620**, 17–26 (2005). https://doi.org/10.1016/j.physletb.2005.06.020. arXiv:hep-ph/0505013

38. A. Boyarsky, M. Ovchynnikov, O. Ruchayskiy, V. Syvolap, Improved big bang nucleosynthesis constraints on heavy neutral leptons. Phys. Rev. D **104**(2), 023517 (2021). https://doi.org/10.1103/PhysRevD.104.023517. arXiv:2008.00749 [hep-ph]

39. K. Bondarenko, A. Boyarsky, J. Klaric, O. Mikulenko, O. Ruchayskiy, V. Syvolap, I. Timiryasov, An allowed window for heavy neutral leptons below the kaon mass. JHEP **07**, 193 (2021). https://doi.org/10.1007/JHEP07(2021)193. arXiv:2101.09255 [hep-ph]

40. P. Colangelo, F. De Fazio, P. Santorelli, E. Scrimieri, Rare $B \rightarrow K^{(*)}$ neutrino anti-neutrino decays at $B$ factories. Phys. Lett. B **395**, 339–344 (1997). https://doi.org/10.1016/S0370-2693(97)00130-5. arXiv:hep-ph/9610297

41. D. Melikhov, N. Nikitin, S. Simula, Right-handed currents in rare exclusive $B \rightarrow (K, K^*)$ neutrino anti-neutrino decays. Phys. Lett. B **428**, 171–178 (1998). https://doi.org/10.1016/S0370-2693(98)00407-9. arXiv:hep-ph/9803269

42. A.J. Buras, J. Girrbach-Noe, C. Niehoff, D.M. Straub, $B \rightarrow K^{(*)}\nu\bar{\nu}$ decays in the Standard Model and beyond. JHEP **02**, 184 (2015). https://doi.org/10.1007/JHEP02(2015)184. arXiv:1409.4557 [hep-ph]

43. C.S. Kim, Y.G. Kim, T. Morozumi, New physics effects in $B \rightarrow K(*)$ neutrino neutrino decays. Phys. Rev. D **60**, 094007 (1999). https://doi.org/10.1103/PhysRevD.60.094007. arXiv:hep-ph/9905528

44. T.M. Aliev, A. Ozpineci, M. Savci, Rare $B \rightarrow K^*\nu\bar{\nu}$ decay beyond standard model. Phys. Lett. B **506**, 77–84 (2001). https://doi.org/10.1016/S0370-2693(01)00365-3. arXiv:hep-ph/0101066

45. R. Bause, H. Gisbert, M. Golz, G. Hiller, Interplay of dineutrino modes with semileptonic rare B-decays. JHEP **12**, 061 (2021). https://doi.org/10.1007/JHEP12(2021)061. arXiv:2109.01675 [hep-ph]

46. J. Gratrex, M. Hopfer, R. Zwicky, Generalised helicity formalism, higher moments and the $B \rightarrow K_{J_K}(\rightarrow K\pi)\bar{\ell}_1\ell_2$ angular distributions. Phys. Rev. D **93**(5), 054008 (2016). https://doi.org/10.1103/PhysRevD.93.054008. arXiv:1506.03970 [hep-ph]

47. R. Bause, H. Gisbert, M. Golz, G. Hiller, Lepton universality and lepton flavor conservation tests with dineutrino modes.

Eur. Phys. J. C **82**(2), 164 (2022). https://doi.org/10.1140/epjc/s10052-022-10113-6. arXiv:2007.05001 [hep-ph]

48. Y. Liao, X.-D. Ma, Operators up to dimension seven in standard model effective field theory extended with sterile neutrinos. Phys. Rev. D **96**(1), 015012 (2017). https://doi.org/10.1103/PhysRevD.96.015012. arXiv:1612.04527 [hep-ph]

49. J. Aebischer, M. Fael, C. Greub, J. Virto, B physics beyond the standard model at one loop: complete renormalization group evolution below the electroweak scale. JHEP **09**, 158 (2017). https://doi.org/10.1007/JHEP09(2017)158. arXiv:1704.06639 [hep-ph]

50. E.E. Jenkins, A.V. Manohar, P. Stoffer, Low-energy effective field theory below the electroweak scale: operators and matching. JHEP **03**, 016 (2018). https://doi.org/10.1007/JHEP03(2018)016. arXiv:1709.04486 [hep-ph]

51. T. Li, X.-D. Ma, M.A. Schmidt, Implication of $K \rightarrow \pi\nu\bar{\nu}$ for generic neutrino interactions in effective field theories. Phys. Rev. D **101**(5), 055019 (2020). https://doi.org/10.1103/PhysRevD.101.055019. arXiv:1912.10433 [hep-ph]

52. T. Li, X.-D. Ma, M.A. Schmidt, General neutrino interactions with sterile neutrinos in light of coherent neutrino-nucleus scattering and meson invisible decays. JHEP **07**, 152 (2020). https://doi.org/10.1007/JHEP07(2020)152. arXiv:2005.01543 [hep-ph]

53. CHARM Collaboration, F. Bergsma et al., A search for decays of heavy neutrinos in the mass range 0.5-GeV to 2.8-GeV. Phys. Lett. B **166**, 473–478 (1986). https://doi.org/10.1016/0370-2693(86)91601-1

54. NuTeV, E815 Collaboration, A. Vaitaitis et al., Search for neutral heavy leptons in a high-energy neutrino beam. Phys. Rev. Lett. **83**, 4943–4946 (1999). https://doi.org/10.1103/PhysRevLett.83.4943. arXiv:hep-ex/9908011

55. DELPHI Collaboration, P. Abreu et al., Search for neutral heavy leptons produced in Z decays. Z. Phys. C **74**, 57–71 (1997). https://doi.org/10.1007/s002880050370 [Erratum: Z. Phys. C 75, 580 (1997)]

56. A.J. Buras, Weak Hamiltonian, CP violation and rare decays, in *Les Houches Summer School in Theoretical Physics, Session 68: Probing the Standard Model of Particle Interactions*, pp. 281–539 (1998). arXiv:hep-ph/9806471

57. J. Brod, M. Gorbahn, E. Stamou, Two-loop electroweak corrections for the $K \rightarrow \pi\nu\bar{\nu}$ decays. Phys. Rev. D **83**, 034030 (2011). https://doi.org/10.1103/PhysRevD.83.034030. arXiv:1009.0947 [hep-ph]

58. D.M. Straub, flavio: a Python package for flavour and precision phenomenology in the Standard Model and beyond. arXiv:1810.08132 [hep-ph]

59. P. Stangl, flav-io/flavio: v2.5.5 (2023). https://doi.org/10.5281/zenodo.7994776

60. Belle Collaboration, R. van Tonder et al., Measurements of $q^2$ moments of inclusive $B \rightarrow X_c\ell^+\nu_\ell$ decays with hadronic tagging. Phys. Rev. D **104**(11), 112011 (2021). https://doi.org/10.1103/PhysRevD.104.112011. arXiv:2109.01685 [hep-ex]

61. N. Gubernari, M. Reboud, D. van Dyk, J. Virto, Dispersive analysis of $B \rightarrow K^{(*)}$ and $B_s \rightarrow \phi$ form factors. arXiv:2305.06301 [hep-ph]

62. A. Bharucha, D.M. Straub, R. Zwicky, $B \rightarrow V\ell^+\ell^-$ in the Standard Model from light-cone sum rules. JHEP **08**, 098 (2016). https://doi.org/10.1007/JHEP08(2016)098. arXiv:1503.05534 [hep-ph]

63. S. Descotes-Genon, A. Khodjamirian, J. Virto, Light-cone sum rules for $B \rightarrow K\pi$ form factors and applications to rare decays. JHEP **12**, 083 (2019). https://doi.org/10.1007/JHEP12(2019)083. arXiv:1908.02267 [hep-ph]

64. J.F. Kamenik, C. Smith, Tree-level contributions to the rare decays $B^+ \rightarrow \pi^+\nu\bar{\nu}$, $B^+ \rightarrow K^+\nu\bar{\nu}$, and $B^+ \rightarrow K^{*+}\nu\bar{\nu}$ in the Standard Model. Phys. Lett. B **680**, 471–475 (2009). https://doi.org/10.1016/j.physletb.2009.09.041. arXiv:0908.1174 [hep-ph]

65. G. Alonso-Álvarez, M. Escudero, The first limit on invisible decays of $B_s$ mesons comes from LEP. arXiv:2310.13043 [hep-ph]

66. Belle-II Collaboration, W. Altmannshofer et al., The Belle II Physics Book, PTEP 2019, no. 12, 123C01 (2019). arXiv:1808.10567 [hep-ex]. [Erratum:PTEP 2020, 029201 (2020)]

67. N. Rajeev, R. Dutta, Consequences of $b \to s\mu + \mu$- anomalies on $B \to K(*)\nu\bar{\nu}$, $Bs \to (\eta, \eta')\nu\bar{\nu}$ and $Bs \to \phi\nu\bar{\nu}$ decay observables. Phys. Rev. D **105**(11), 115028 (2022). https://doi.org/10.1103/PhysRevD.105.115028. arXiv:2112.11682 [hep-ph]

68. N. Das, R. Dutta, New physics analysis of $\Lambda_b \to (\Lambda^*(\to pK^-), \Lambda(\to p\pi))(\mu^+\mu^-, \nu\bar{\nu})$ baryonic decays under SMEFT framework. arXiv:2307.03615 [hep-ph]

69. M. Bordone, M. Rahimi, K.K. Vos, Lepton flavour violation in rare $\Lambda_b$ decays. Eur. Phys. J. C **81**(8), 756 (2021). https://doi.org/10.1140/epjc/s10052-021-09531-9. arXiv:2106.05192 [hep-ph]

70. L. Li, M. Ruan, Y. Wang, Y. Wang, Analysis of $Bs \to \phi\nu\bar{\nu}$ at CEPC. Phys. Rev. D **105**(11), 114036 (2022). https://doi.org/10.1103/PhysRevD.105.114036. arXiv:2201.07374 [hep-ph]

71. Y. Amhis, M. Kenzie, M. Reboud, A.R. Wiederhold, Prospects for searches of $b \to s\nu\bar{\nu}$ decays at FCC-ee. arXiv:2309.11353 [hep-ex]

72. B. Bhattacharya, T.E. Browder, Q. Campagna, A. Datta, S. Dubey, L. Mukherjee, A. Sibidanov, Implications for the $\Delta A_{FB}$ anomaly in $\bar{B}^0 \to D^{*+}\ell^-\bar{\nu}$ using a new Monte Carlo event generator. Phys. Rev. D **107**(1), 015011 (2023). https://doi.org/10.1103/PhysRevD.107.015011. arXiv:2206.11283 [hep-ph]

73. N. Gubernari, A. Kokulu, D. van Dyk, $B \to P$ and $B \to V$ form factors from $B$-meson light-cone sum rules beyond leading twist. JHEP **01**, 150 (2019). https://doi.org/10.1007/JHEP01(2019)150. arXiv:1811.00983 [hep-ph]

74. Belle Collaboration, R. Glattauer et al., Measurement of the decay $B \to D\ell\nu_\ell$ in fully reconstructed events and determination of the Cabibbo–Kobayashi–Maskawa matrix element $|V_{cb}|$. Phys. Rev. D **93**(3), 032006 (2016). https://doi.org/10.1103/PhysRevD.93.032006. arXiv:1510.03657 [hep-ex]

75. Belle-II Collaboration, L. Aggarwal et al., Test of light-lepton universality in the rates of inclusive semileptonic B-meson decays at Belle II. Phys. Rev. Lett. **131**(5), 051804 (2023). https://doi.org/10.1103/PhysRevLett.131.051804. arXiv:2301.08266 [hep-ex]

76. M. Rahimi, K.K. Vos, Standard Model predictions for lepton flavour universality ratios of inclusive semileptonic B decays. JHEP **11**, 007 (2022). https://doi.org/10.1007/JHEP11(2022)007. arXiv:2207.03432 [hep-ph]

77. A. Greljo, J. Martin Camalich, J.D. Ruiz-Álvarez, Mono-$\tau$ signatures at the LHC constrain explanations of $B$-decay anomalies. Phys. Rev. Lett. **122**(13), 131803 (2019). https://doi.org/10.1103/PhysRevLett.122.131803. arXiv:1811.07920 [hep-ph]

78. T. Han, J. Liao, H. Liu, D. Marfatia, Right-handed Dirac and Majorana neutrinos at Belle II. JHEP **04**, 013 (2023). https://doi.org/10.1007/JHEP04(2023)013. arXiv:2207.07029 [hep-ph]

79. J. De Vries, H.K. Dreiner, J.Y. Günther, Z.S. Wang, G. Zhou, Long-lived sterile neutrinos at the LHC in effective field theory. JHEP **03**, 148 (2021). https://doi.org/10.1007/JHEP03(2021)148. arXiv:2010.07305 [hep-ph]

80. G. Zhou, J.Y. Günther, Z.S. Wang, J. de Vries, H.K. Dreiner, Long-lived sterile neutrinos at Belle II in effective field theory. JHEP **04**, 057 (2022). https://doi.org/10.1007/JHEP04(2022)057. arXiv:2111.04403 [hep-ph]

81. R. Beltrán, G. Cottin, J.C. Helo, M. Hirsch, A. Titov, Z.S. Wang, Long-lived heavy neutral leptons from mesons in effective field theory. JHEP **01**, 015 (2023). https://doi.org/10.1007/JHEP01(2023)015. arXiv:2210.02461 [hep-ph]

82. Belle-II Collaboration, L. Aggarwal et al., Snowmass White Paper: Belle II physics reach and plans for the next decade and beyond. arXiv:2207.06307 [hep-ex]

83. R. Beltrán, R. Cepedello, M. Hirsch, Tree-level UV completions for $N_R$ SMEFT d = 6 and d = 7 operators. JHEP **08**, 166 (2023). https://doi.org/10.1007/JHEP08(2023)166. arXiv:2306.12578 [hep-ph]

84. I. Doršner, S. Fajfer, A. Greljo, J.F. Kamenik, N. Košnik, Physics of leptoquarks in precision experiments and at particle colliders. Phys. Rep. **641**, 1–68 (2016). https://doi.org/10.1016/j.physrep.2016.06.001. arXiv:1603.04993 [hep-ph]

85. J. de Blas, J.C. Criado, M. Perez-Victoria, J. Santiago, Effective description of general extensions of the Standard Model: the complete tree-level dictionary. JHEP **03**, 109 (2018). https://doi.org/10.1007/JHEP03(2018)109. arXiv:1711.10391 [hep-ph]

86. J.D. Hunter, Matplotlib: a 2d graphics environment. Comput. Sci. Eng. **9**(3), 90–95 (2007). https://doi.org/10.1109/MCSE.2007.55